HAL
open science

# Analysis of HighDimensional Signal Data by Manifold Learning and Convolutions

Mijail Guillemard, Armin Iske

## To cite this version:

Mijail Guillemard, Armin Iske. Analysis of HighDimensional Signal Data by Manifold Learning and Convolutions. SAMPTA'09, May 2009, Marseille, France. pp.General session. hal-00453449

**HAL Id: hal-00453449**

**https://hal.science/hal-00453449v1**

Submitted on 4 Feb 2010

**HAL** is a multi-disciplinary open access archive for the deposit and dissemination of scientific research documents, whether they are published or not. The documents may come from teaching and research institutions in France or abroad, or from public or private research centers.

L'archive ouverte pluridisciplinaire **HAL**, est destinée au dépôt et à la diffusion de documents scientifiques de niveau recherche, publiés ou non, émanant des établissements d'enseignement et de recherche français ou étrangers, des laboratoires publics ou privés.

# Analysis of High-Dimensional Signal Data by Manifold Learning and Convolutions

Mijail Guillemard (1) and Armin Iske (1)

(1) Department of Mathematics, University of Hamburg, D-20146 Hamburg, Germany.
guillemard@math.uni-hamburg.de, iske@math.uni-hamburg.de

## Abstract:

A novel concept for the analysis of high-dimensional signal data is proposed. To this end, customized techniques from manifold learning are combined with convolution transforms, being based on wavelets. The utility of the resulting method is supported by numerical examples concerning low-dimensional parameterizations of scale modulated signals and solutions to the wave equation at varying initial conditions.

## 1. Introduction

Recent advances in nonlinear dimensionality reduction and manifold learning have provided new methods for the analysis of high-dimensional signals. In this problem, a very large data set $U \subset \mathbb{R}^n$ of scattered points is given, where the data points are assumed to lie on a compact submanifold $\mathcal{M}$ of $\mathbb{R}^n$, i.e. $U \subset \mathcal{M} \subset \mathbb{R}^n$. Moreover, the dimension $k = \dim(\mathcal{M})$ of $\mathcal{M}$ is assumed to be much smaller than the dimension of the ambient space $\mathbb{R}^n$, $k \ll n$. Now, the primary goal in the dimensionality reduction is the construction of a low-dimensional representation of the data $U$.

In this paper, a novel concept for signal data analysis through dimensionality reduction is proposed. To this end, suitable techniques from manifold learning are combined with convolution transforms. Moreover, another important ingredient is a (suitable) projection map $P : \mathbb{R}^n \to \mathbb{R}^k$ that finally outputs the desired low-dimensional representation for $U$. Note that for the sake of approximation quality, we need to preserve intrinsic geometrical and topological properties of the manifold $\mathcal{M}$, and so the construction of the composite dimensionality reduction method requires particular care. In the proposed data analysis, the geometric distortion of the manifold, being incurred by the chosen convolution transform, plays a key role.

We remark that similar concepts from differential geometry are enjoying increasing interest in related applications of sampling theory, including surface reconstruction in reverse engineering and image analysis [5]. Further related concepts can be found in classical dimensionality reduction schemes, such as in *principal component analysis* and *multidimensional scaling*, while more recent techniques are including *Isomap* and *LLE methods* [4, 7] *Local Tangent Space Alignment* (LTSA) [6], *Sample Logmaps* [1], and, most recently, *Riemannian Normal Coordinates* [2, 3].

The outline of the paper is as follows. In the following Section 2, the main ingredients of the proposed nonlinear dimensionality reduction scheme, especially the construction of the convolution and projection map, are explained. Then, in Section 3 relevant aspects concerning distortion analysis are addressed. Finally, Section 4 shows the good performance of the resulting nonlinear dimensionality reduction method. To this end, numerical examples concerning low-dimensional parameterization of scale modulated signals and solutions to the wave equation at varying initial conditions are illustrated.

## 2. Construction of the Data Analysis

Given a set of signals $U = \{u_i\}_{i=1}^m \subset \mathcal{M}$, that we assume to lie in (or near) a low-dimensional Riemannian compact submanifold $\mathcal{M}$, of $\mathbb{R}^n$, we wish to analyse the given data for the purpose of dimensionality reduction. Therefore, we assume that there is an embedding $A : \Omega \to \mathcal{M}$, giving a parameterization of $\mathcal{M}$, where the domain $\Omega \subset \mathbb{R}^d$ lies in a low-dimensional Euclidean space $\mathbb{R}^d$, i.e., $d \ll n$. But the parameter domain $\Omega$ is unknown. Therefore, the goal of dimensionality reduction is to find a sufficiently accurate approximation $\Omega'$ of $\Omega$, through which the desired low-dimensional representation for $U$ is obtained.

We remark that the construction of the data analysis is required to depend on intrinsic geometrical and topological properties of the manifold $\mathcal{M}$. To this end, we apply a particular convolution transform $T : \mathcal{M} \to \mathcal{M}_T$, $\mathcal{M}_T = \{T(p) \ : p \in \mathcal{M}\}$, to each of the data sites $u_i$, followed by a suitable projection $P : \mathcal{M}_T \to \Omega'$, yielding a nonlinear data transformation for dimensionality reduction. The following diagram reflects our concept.

$$\begin{array}{ccc} \Omega \subset \mathbb{R}^d & \xrightarrow{A} & U \subset \mathcal{M} \subset \mathbb{R}^n \\ & & \downarrow T \\ \Omega' \subset \mathbb{R}^d & \xleftarrow[P]{} & U_T \subset \mathcal{M}_T \subset \mathbb{R}^n \end{array} \tag{1}$$

Note that both the construction of the transformation $T$ and the projection need particular care. Indeed, in order to maintain the intrinsic geometrical properties of the manifold $\mathcal{M}$, it is required to investigate the curvature distortion of $\mathcal{M}$ under the transform $T$. For this purpose, convolution filters are powerful tools for the construction of

suitable signal transforms $T$. This is supported by our numerical results in Section 4., where wavelet transforms are used for a customized construction of $T$.
Finally, let us remark that standard methods in signal processing rely on on special characteristics of a discrete-time signal $u_k \in \mathbb{R}^n$, such as frequency content, time duration, phase and amplitude information, etc. In typical application scenarios, signal data are not just isolated items of information, but they are rather incorporating correlations reflecting characteristic properties of the sampled object. Therefore, when designing customized signal transforms, one should exploit available context information on characteristic properties of the target object in order to improve the quality of the data analysis. In our particular application scenario, special emphasis needs to be placed on intrinsic geometrical properties of the manifold $\mathcal{M}$, where a preprocessing distortion analysis of the curvature is of vital importance.

## 3. Curvature Distortion Analysis

Our main objective is to estimate the curvature distortion in the geometry of the manifold $\mathcal{M}$ incurred by the application of the linear transformation $T : \mathcal{M} \to \mathcal{M}_T$, where $T$ may, for instance, representing a wavelet or a convolution filter. To this end, we first need to evaluate relevant effects on the geometrical deformation of $\mathcal{M}$ under various specific transformations $T$. This then amounts to constructing suitable transformations $T$ which are well-adapted to the characteristic properties of the specific data. Preferable choices for $T : \mathcal{M} \to \mathcal{M}_T$ are diffeomorphisms, in which case $\dim(\mathcal{M}) = \dim(\mathcal{M}_T)$.

### 3.1 Sectional Curvature Distortions

In general, a fundamental invariant of a manifold with respect to its isometries are the sectional curvatures. This concept is derived from the idea of the Gaussian curvature in the setting of 2-manifolds, and is defined as

$$K_{\mathcal{M}} = \frac{< R(X,Y)Y, X >}{\|X\|^2\|Y\|^2 - < X, Y >^2},$$

for the *curvature tensor* $R$, defined for a triple of smooth vector fields $X, Y, Z$ as

$$R(X,Y)Z = \nabla_X \nabla_Y Z - \nabla_Y \nabla_X Z - \nabla_{[X,Y]} Z.$$

We recall that the affine connection (a Levi-Cevita connection for our situation) is a bilinear map

$$\nabla : C^\infty(\mathcal{M}, T\mathcal{M}) \times C^\infty(\mathcal{M}, T\mathcal{M}) \to C^\infty(\mathcal{M}, T\mathcal{M})$$

that can be expressed with the Christoffel symbols defined, for a particular system of local coordinates $(x_1, \ldots, x_n)$, as $\nabla_{\partial_i}\partial_j = \sum_{k=1}^n \Gamma_{ij}^k \partial_k$. The Christoffel symbols can be described with respect to the metric tensor via

$$\Gamma_{ij}^k = \frac{1}{2}\sum_{\ell=1}^m \left( \frac{\partial g_{j\ell}}{\partial x_i} + \frac{\partial g_{i\ell}}{\partial x_j} + \frac{\partial g_{ij}}{\partial x_\ell} \right) g^{\ell k}.$$

In order to estimate the distortion caused by the linear map $T : \mathcal{M} \to \mathcal{M}_T$, we compare the Gaussian curvatures between $\mathcal{M}$ and $\mathcal{M}_T$, denoted respectively $K_{\mathcal{M}}$, and $K_{\mathcal{M}_T}$,

$$D_K^T(p) = K_{\mathcal{M}}(p) - K_{\mathcal{M}_T}(T(p)) \quad \text{for } p \in \mathcal{M}.$$

If $T$ is invertible, then the Gaussian curvature $K_{\mathcal{M}_T}$ in $\mathcal{M}_T$ can be computed as a function of the metric $g$ in $\mathcal{M}$ by using a *pullback* of the curvature tensor $R$ in $\mathcal{M}$ with respect to the inverse map $T^{-1} : \mathcal{M}_T \to \mathcal{M}$, or, equivalently, by using a *pushforward* of the curvature tensor $R$ in $\mathcal{M}$ with respect to $T : \mathcal{M} \to \mathcal{M}_T$. An alternative strategy is to consider the composition of $T$ with a particular system of local coordinates $(x_1, \ldots, x_n)$ of $\mathcal{M}$, along with the metric tensor

$$g_{ij}(p) = g_{ij}(x_1, \ldots, x_m) = \left\langle \frac{\partial}{\partial x_i}, \frac{\partial}{\partial x_j} \right\rangle.$$

When considering the linear transformation $T$ representing the convolution filter, an important case is when $T$ is represented by a Toeplitz matrix, with filter coefficients $H = (h_1, \ldots, h_m)$, i.e.,

$$T = \begin{bmatrix} h_1 & 0 & \ldots & 0 \\ h_2 & h_1 & \ldots & 0 \\ \vdots & \vdots & \ldots & \vdots \\ h_m & h_{m-1} & \ldots & h_1 \\ 0 & h_m & \ldots & h_2 \\ \vdots & \vdots & \ldots & \vdots \\ 0 & 0 & \ldots & h_m \end{bmatrix}.$$

Note that the curvature distortion caused by the map $T$ will be controlled by the singular values of $T$, which due to the Toeplitz matrix structure, are obtained from the Fourier coefficients of $H$.
Now, our primary objective is to investigate the influence of the filter coefficients in $H$ on the curvature distortion $D_K^T$. Moreover, we study filters being required to obtain a given curvature distortion. The latter is particularly useful for the adaptive construction of a low dimensional representation of $U$.

### 3.2 Curvature Distortions for Curves

As for the special case of a curve $r : I = [t_0, t_1] \to \mathbb{R}^m$, with arc-length parameterization $s(a,t) = \int_a^t \|r'(x)\|\, dx$, recall that the curvature of $r$ is $k(s) = \|r''(s)\|$. For an arbitrary parameterizations of $r$, its curvature is given by

$$K^2 = \frac{\|\ddot{r}\|^2\|\dot{r}\|^2 - < \ddot{r}, \dot{r} >^2}{(\|\dot{r}\|^2)^3}.$$

In the remainder of this section, we briefly discuss the curvature distortion under linear maps (e.g. convolution transform) and under smooth maps. To compute the curvature distortion of a curve $r : I = [t_0, t_1] \to \mathbb{R}^m$ under a linear map $T$, we consider the curvature of $r_T = \{Tr(t), t \in I\}$, computed as follows.

$$K_T^2 \equiv K_T^2(t) = \frac{\|T\ddot{r}\|^2\|T\dot{r}\|^2 - < T\ddot{r}, T\dot{r} >^2}{(\|T\dot{r}\|^2)^3}. \quad (2)$$

As for the general case of smooth maps $F : \mathbb{R}^m \to \mathbb{R}^r$, the curvature distortion can be approximated by using the

Jacobian matrix $J_F$ and its singular value decomposition,

$$\begin{aligned} J_F(p) &= \begin{bmatrix} \frac{\partial f_1}{\partial x_1}(p) & \cdots & \frac{\partial f_1}{\partial x_m}(p) \\ \vdots & \ddots & \vdots \\ \frac{\partial f_r}{\partial x_1}(p) & \cdots & \frac{\partial f_r}{\partial x_m}(p) \end{bmatrix} \\ &= U_F(p) D_F(p) V_F^T(p) \qquad \text{for } p \in \mathcal{M}. \end{aligned}$$

The curvature distortion of a curve $r : [t_0, t_1] \to \mathbb{R}^m$ under $F$ can in this case be analyzed through the expression

$$K_F^2 \equiv K_F^2(p) = \frac{\|J_F \ddot{r}\|^2 \|J_F \dot{r}\|^2 - < J_F \ddot{r}, J_F \dot{r} >^2}{(\|J_F \dot{r}\|^2)^3},$$

where, unlike in the linear case (2), the Jacobian matrices $J_F$ depend on $p \in \mathcal{M}$.

## 4. Numerical Examples

This section presents three different numerical examples to illustrate basic properties of the proposed analysis of high-dimensional signal data. Further details shall be discussed during the conference.

### 4.1 Low-dimensional parameterization of scale modulated signals

In this example, we illustrate the geometrical effect of a convolution transform for a set of functions lying on a curve embedded in a high dimensional space. More precisely, we analyze a scale modulated family of functions $U \subset \mathbb{R}^{64}$, parameterized by three values in $\Omega \subset \mathbb{R}^3$,

$$U = \left\{ f_{\alpha(t)} = \sum_{i=1}^{3} e^{-\alpha_i(t)(\cdot - b_i)^2} : \alpha(t) \in \Omega \right\}.$$

The parameter set for the scale modulation is given by the curve

$$\Omega = \left\{ \alpha(t) = (\alpha_1(t), \alpha_2(t), \alpha_3(t))^T \in \mathbb{R}^3, \ : t \in [t_0, t_1] \right\}.$$

Figure 1 (left) shows the parameter domain $\Omega$, a star shaped curve in $\mathbb{R}^3$. A PCA projection in $\mathbb{R}^3$, applied to the set $U \subset \mathbb{R}^{64}$, is also displayed in Figure 1 (middle). The projection illustrates the curvature distortion caused by the nonlinear map $A : \Omega \subset \mathbb{R}^3 \to U \subset \mathbb{R}^{64}$, $A(\alpha(t)) = f_{\alpha(t)}$.

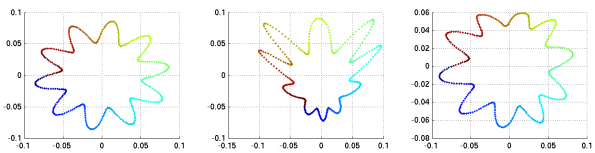

Figure 1: Parameter set $\Omega \subset \mathbb{R}^3$, data $U \subset \mathbb{R}^{64}$, and wavelet correction $T(U) \subset \mathbb{R}^{64}$.

Finally, Figure 1 (right), shows the resulting data transformation $T(U)$ using a Daubechies wavelet w.r.t. a specific band of the multiresolution analysis, resulting in a filtering process for each element in $U$. The resulting $T(U)$, presents a curvature correction that recovers the original geometry of $\Omega$ fairly well.

To explain the resulting curvature correction, we need to analyze the singular values and singular vectors of the convolution map $T$. In fact, the singular values of $T$ can be viewed as scaling factors (stretching or shrinking) along corresponding axis in the (local) embedding of $U$. Moreover, the spectrum of $T$ depends on the particular filter design.

### 4.2 Low dimensional parameterization of wave equation solutions

In this second example, we regard the one-dimensional wave equation

$$\frac{\partial u}{\partial t} = c^2 \frac{\partial u}{\partial x}, \quad 0 < x < 1, \ t \geq 0, \tag{3}$$

with initial conditions

$$u(0, x) = f(x), \ \frac{\partial u}{\partial t}(0, x) = g(x), \quad 0 \leq x \leq 1. \tag{4}$$

We make use of the previous example to construct a set of initial values (i.e. functions) parameterized by a star shaped curve $U_0 = U$. Our objective is to investigate the distortion caused by the evolution $U_t$ of the solutions on given initial values $U_0$. Recall that the evolution of the wave equation is constituted by the set of solutions

$$\begin{aligned} U_t \quad = \quad & \{u_\alpha \equiv u_\alpha(t, x) : u_\alpha \text{ satisfying (3) with} \\ & \text{initial condition } f \equiv f_\alpha \text{ in (4) for } \alpha \in \Omega\}. \end{aligned}$$

Now, the solution of the wave equation can numerically be computed by using finite differences, yielding the iteration

$$u^{(j+1)} = A u^{(j)} + b^{(j)},$$

where for $\mu = \gamma \Delta t / (\Delta x)^2$, the iteration matrix is given by

$$A = \begin{bmatrix} 1-2\mu & \mu & & & & \\ \mu & 1-2\mu & \mu & & & \\ & \mu & 1-2\mu & \mu & & \\ & & \ddots & \ddots & \ddots & \\ & & & 0 & \mu & 1-2\mu \end{bmatrix}.$$

Recall that in the convergence analysis of the iteration, which can be rewritten as,

$$\begin{aligned} u^{(j+2)} &= A u^{(j+1)} + b^{(j+1)} \\ &= A(A u^{(j)} + b^{(j)}) + b^{(j+1)} \\ &= A^{(2)} u^{(j)} + A b^{(j)} + b^{(j+1)}, \end{aligned}$$

the spectrum of the matrices $A^k$ play a key role. In fact, due to the decomposition $A^k = U D^k U^T$, the geometrical distortion in the evolution of $U_t$ depends on the evolution of the eigenvalues of $A$.

### 4.3 Topological Distortion via Filtering

In this final example, we illustrate one relevant phenomenon concerning the topological distortion caused by

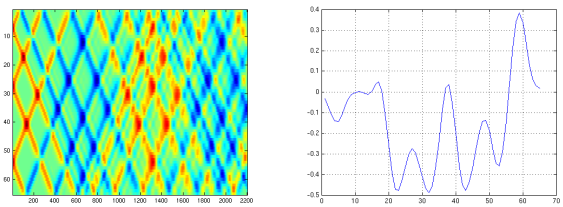

Figure 2: One solution of the wave equation $u(t,x)$ and one measurement $u(t_k,x)$, $t_k = 20$.

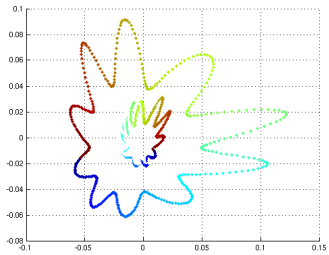

Figure 3: Curvature distortion of the initial manifold under the evolution of the wave equation. The outer curve represents the initial conditions $U_0$ while the inner curve reflects the corresponding solutions $U_t$ for some time $t$.

the utilized convolution transformation. In this couple of two test cases, we take one 1-torus $\Omega_1 \subset \mathbb{R}^3$ and one 2-torus $\Omega_2 \subset \mathbb{R}^3$ as parameter space, respectively. As in the previous examples, we generate a corresponding set of scale modulation functions $U_1$ and $U_2$ (see Figure 4), using $\Omega_1$ and $\Omega_2$ as parameter domains. This gives, for $j = 1, 2$, two different data sets

$$U_j = \left\{ f_{\alpha^j(t)} = \sum_{i=1}^{3} e^{-\alpha_i^j(t)(\cdot - b_i^j)^2} : \alpha^j(t) \in \Omega_j \right\}.$$

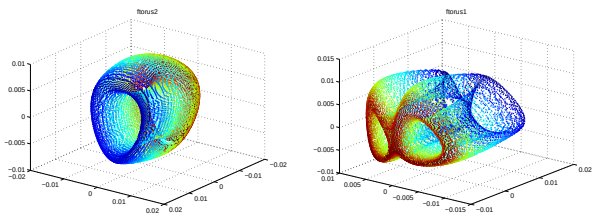

Figure 4: PCA projections of $U_1, U_2 \subset \mathbb{R}^{64}$ onto $\mathbb{R}^3$, generated by $\Omega_1, \Omega_2 \subset \mathbb{R}^3$, two tori of genus 1 and 2.

Now we combine the set $U_1$ and $U_2$ by

$$U = \left\{ f_t = f_{\alpha^1(t)} + f_{\alpha^2(t)} : \alpha^1(t) \in \Omega_1, \alpha^2(t) \in \Omega_2 \right\}.$$

The resulting projection of the data $U$ is shown in Figure 5. For the purpose of illustration, we recover the sets $U_1$ and $U_2$ from $U$. Note that this is a rather challenging task, especially since the genus of surfaces $U_1$ and $U_2$ are different. Figure 6 shows the reconstructions of the two surfaces $U_1$ and $U_2$. Note that the both the geometrical and topological properties of $U_1$ and $U_2$ are recovered fairly well, which supports the good performance of our convolution transform yet once more. The reconstruction of the utilized convolution involves a selection of suitable bands from the corresponding wavelet multiresolution decomposition. Further details on this shall be explained during the conference.

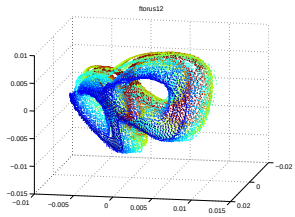

Figure 5: PCA projection of $U \subset \mathbb{R}^{64}$ onto $\mathbb{R}^3$.

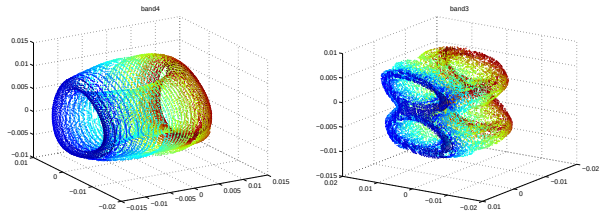

Figure 6: Reconstruction of $U_1$ (left), $U_2$ (right) from $U$.

## 5. Acknowledgments

The authors were supported by the priority program DFG-SPP 1324 of the *Deutsche Forschungsgemeinschaft.*

## References:


[1] A. Brun, C. Westin, M. Herberthsson, and H. Knutsson. Sample logmaps: Intrinsic processing of empirical manifold data. *Proceedings of the (SSBA) Symposium on Image Analysis*, 1, 2006.

[2] A. Brun, C.-F. Westin, M. Herberthson, and H. Knutsson. Fast manifold learning based on riemannian normal coordinates. In *Proceedings of the SCIA;05*, pages 920–929, Joensuu, Finland, June 2005.

[3] T. Lin, H. Zha, and S.U. Lee. Riemannian Manifold Learning for Nonlinear Dimensionality Reduction. *Lecture Notes in Computer Science*, 3951:44, 2006.

[4] S.T. Roweis and L.K. Saul. Nonlinear Dimensionality Reduction by Locally Linear Embedding, 2000.

[5] E. Saucan, E. Appleboim, and Y.Y. Zeevi. Sampling and Reconstruction of Surfaces and Higher Dimensional Manifolds. *Journal of Mathematical Imaging and Vision*, 30(1):105–123, 2008.

[6] H. Zha and Z. Zhang. Principal Manifolds and Nonlinear Dimension Reduction via Local Tangent Space Alignment. *SIAM Journal of Scientific Computing*, 26(1):313–338, 2004.

[7] H. Zha and Z. Zhang. Continuum Isomap for manifold learnings. *Computational Statistics and Data Analysis*, 52(1):184–200, 2007.